Journal of Hazardous Materials, 34 (1993) 81–98
Elsevier Science Publishers B.V., Amsterdam

Computation of natural gas pipeline rupture problems using the method of characteristics

J.A. Olorunmaiye[a,*] and N.E. Imide[b]

[a] *Department of Mechanical Engineering, University of Ilorin, P.M.B. 1515, Ilorin (Nigeria)*
[b] *Department of Mechanical Engineering, Abubakar Tafawa Balewa University, Bauchi (Nigeria)*

(Received July 4, 1992; accepted in revised form December 2, 1992)

Abstract

The flow in a long, high pressure, natural gas pipeline following sudden rupture was modelled as unsteady one-dimensional isothermal flow. The set of hyperbolic partial differential equations were solved with a numerical method of characteristics. The accuracy of the numerical scheme when using linear characteristics with quadratic interpolation was found to be adequate. It was also found that the effect of the curvature of characteristics in isothermal flow was not as pronounced as it was reported in adiabatic flow by Flatt. To assess the hazard of a natural gas pipeline rupture, it is necessary to know the rate of outflow of the gas at the breakpoint as a function of time. The predicted mass flow rate of gas out of the broken end was 18% lower than that predicted using adiabatic flow theory, whereas, there was good agreement with the results of earlier workers who also used isothermal flow theory whose computation method was based on weighted residuals.

1. Introduction

Transient pressure fluctuations in gas pipelines are usually initiated by sudden opening or closure of valves or by compressors. They involve transmittal and reflection of pressure waves in the piping system and may result in pipe rupture from excessive pressure.

The unsteady flow of a gas in a long pipeline after an accidental rupture is of considerable interest to the gas industry because the pipeline contains an enormous amount of flammable gas and a break in it represents a considerable hazard. It is necessary to know the rate of loss of gas from the break to calculate the dispersion range and ground concentration of the air–gas mixture. After rupture, the flow in the low pressure segment of the pipeline is more complex than that in the high pressure segment since the expansion waves entering the pipeline cause flow reversal in the case of the flow in the low

* To whom correspondence should be sent.

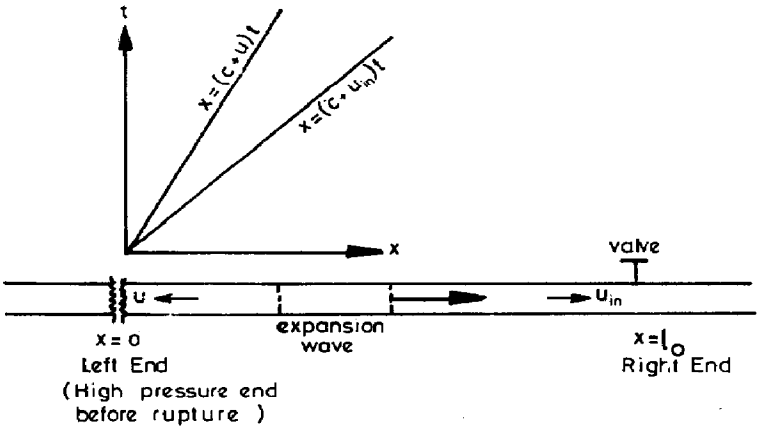

Fig. 1. Physical situation of the problem showing an expansion wave entering the pipeline after rupture.

pressure segment. In Fig. 1, it is assumed that the rupture is equal to the pipe cross-sectional area and immediately to the left of the rupture (in the high pressure segment of the pipeline) a valve is closed completely at the instant of rupture.

Fanneløp and Ryhming [1] studied the unsteady flow in a natural gas pipeline in which a break occurred at the high pressure end. They divided the flow into three time regimes. The "early time" regime following the sudden break is dominated by wave processes and the pressure at the open end approaches the ambient value. This is followed by the "intermediate time regime" in which an internal pressure peak occurs, the location of which corresponds approximately with the location of flow reversal where the velocity is zero. By the time the pressure peak gets to the low pressure end of the pipe (the closed end), the "late time" regime starts. In this time regime, the pressure in the pipeline decreases monotonically from the closed end of the pipe to the open end.

They used an integral method to analyse the unsteady flow in the pipeline assuming the flow to be isothermal. They ignored inertia terms in the equations to obtain a set of parabolic equations. Their method could not handle the early time regime and it gave no information on the internal flow because spatial distributions in the range $x=0$ to $x=l_0$ were assumed for the pressure and pressure–velocity product to obtain solutions.

Lang and Fanneløp [2] improved on this work by using some approximation procedures in the family of weighted residuals. The flow profiles were not specified *a priori* as in the work of Fanneløp and Ryhming but were found as part of the solution. They were able to obtain more accurate results but their methods produced oscillations in the dependent variables predicted during the early time regime.

Ryhming [3] used the method of matched asymptotic expansion to study unsteady isothermal flow in a long pipeline ruptured suddenly. He showed that wall friction caused the velocity derivative along the pipe to become singular at the broken end exit when the flow there was critical. His composite first order solution gave velocity profile in the pipeline at various times. Since his analysis concentrated on predicting the velocity profile and did not include pressure or density variations in the pipe, it could not be used to predict the flow rate out of the pipe during the early time regime.

Flatt [4] developed a method of characteristics to compute unsteady adiabatic flow of natural gas in a long pipeline following a sudden break. Since he used the full set of hyperbolic partial differential equations, his method could handle flows in the three time regimes.

However, with high pressure variations such as occur in pipeline break problems, heat transfer between the fluid and the medium surrounding the pipe will be appreciable unless the pipe is lagged. In fact, the flow process is expected to be closer to isothermal than adiabatic flow due to compensating errors in density and critical velocity that occur in the former. The present effort is directed at developing a numerical method of characteristics to solve the set of hyperbolic partial differential equations describing unsteady isothermal flow following a break in a long pipeline. It therefore compliments the works of Ryhming, Fanneløp and Lang in supplying the missing information in their analysis during the early time regime. It also has the advantage of being applicable to the three flow time regimes.

Flatt [4] did not apply his adiabatic flow model to predict the flow up to the late time regimes because of the long computer time it would take. Since the set of equations for isothermal flow (two equations) is simpler than that for adiabatic flow (three equations) computation time will be less of a problem in this case of the former type, thereby making it less expensive for computing the flow for all the time regimes.

2. Mathematical model

For one-dimensional flow in a pipe of uniform diameter, the conservation equations for mass and momentum are

$$\frac{\partial \rho}{\partial t}+u\frac{\partial \rho}{\partial x}+\rho\frac{\partial u}{\partial x}=0 \tag{1}$$

$$\frac{\partial u}{\partial t}+u\frac{\partial u}{\partial x}+\frac{1}{\rho}\frac{\partial P}{\partial x}+F=0 \tag{2}$$

where

$$F=\frac{2f}{d}u|u| \tag{3}$$

and u^2 being expressed as $u|u|$ to ensure that the frictional force shall always act opposite to the direction of motion.

The equation of state for isothermal flow of a perfect gas is

$$P=\rho RT_0 \tag{4}$$

Eliminating density, ρ, from eqs. (1) and (2) using (4), the continuity and momentum equations become

$$\frac{\partial p}{\partial t}+u\frac{\partial p}{\partial x}+P\frac{\partial u}{\partial x}=0 \tag{5}$$

and

$$\frac{\partial u}{\partial t}+u\frac{\partial u}{\partial x}+\frac{c^2}{P}\frac{\partial P}{\partial x}+F=0 \tag{6}$$

where the expression for isothermal speed of sound

$$c^2=RT_0 \tag{7}$$

has been used.

Although the isothermal speed of sound does not change, the expansion wave will fan out as shown in Fig. 1 because the head of the wave travels in fluid particles having positive velocity, whereas the tail travels at velocity c relative to particles having negative velocity.

Choosing the length of the pipe, isothermal speed of sound, the ambient pressure and temperature as the reference parameters, the non-dimensional forms of eqs. (5) and (6) are:

$$\frac{\partial P'}{\partial Z}+P'\frac{\partial U}{\partial X}+U\frac{\partial P'}{\partial X}=0 \tag{8}$$

$$\frac{\partial U}{\partial Z}+U\frac{\partial U}{\partial X}+\frac{1}{P'}\frac{\partial P'}{\partial X}=-F' \tag{9}$$

3. Numerical method

Equations (8) and (9) constitute a set of quasi-linear hyperbolic partial differential equations which can be solved using the method of characteristics. Hartree's hybrid scheme which was used earlier by Olorunmaiye and Kentfield [5] is also used in this work. In this method, a rectangular grid is imposed on the integration domain and the equations are integrated along the characteristics directions. The dependent variables here are P and U.

The characteristic curves of eqs. (8) and (9) are given by

$$\frac{dX}{dZ}=U\pm 1 \tag{10}$$

Equation (10) gives the downstream and upstream propagation directions in the X–Z plane, of a pressure wave travelling at the isothermal speed of sound relative to the fluid.

The compatibility equations along the characteristics having reciprocal slopes $(U+1)$ and $(U-1)$, respectively, are

$$\frac{1}{P'}\frac{\delta_+ P'}{\delta Z}+\frac{\delta_+ U}{\delta Z}+F'=0 \tag{11}$$

$$-\frac{1}{P'}\frac{\delta_- P'}{\delta Z}+\frac{\delta_- U}{\delta Z}+F'=0 \tag{12}$$

The characteristics reaching a grid point for different flow velocities are shown in Fig. 2. The characteristics having reciprocal slopes $(U+1)$ and $(U-1)$ are labelled OV and TV, respectively. The finite difference approximation of eqs. (11) and (12) are

$$U_V-U_O+(\ln P'_V-\ln P'_O)=-F'_{OV}\Delta Z \tag{13}$$

$$U_V-U_T-(\ln P'_V-\ln P'_T)=-F'_{TV}\Delta Z \tag{14}$$

Rearranging eqs. (13) and (14) gives

$$P'_V=\exp\left[\tfrac{1}{2}\{(F'_{TV}\Delta Z-F'_{OV}\Delta Z+U_O-U_T+\ln P'_T+\ln P'_O)\}\right] \tag{15}$$

The double subscripts on a term indicates that the term is taken to be the mean of its value at the end points indicated by the two subscripts (See Fig. 2).

4. Boundary conditions

For flow with velocity $|U|\leqslant 1$, only characteristic OV reaches the grid point at the right end whereas only characteristics TV reaches the grid point at the left end.

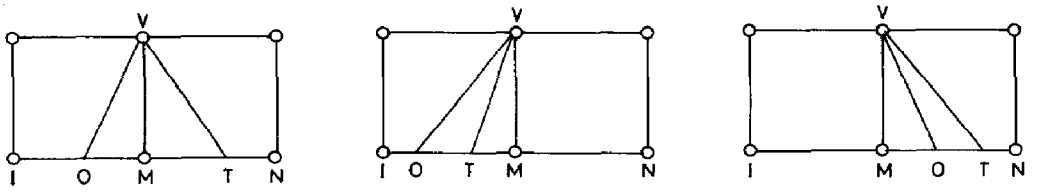

(a) Flow with $|u|<1$ (b) Flow to the right with $|u|>1$ (c) Flow to the left with $|u|>1$

Fig. 2. Characteristics reaching an internal grid points.

4.1 Right end

Assuming the change causing unsteady flow in the pipeline happens at the left end as in Fig. 1, the pressure and velocity at the right end is not affected until Z^* when the wave reaches there. Hence,

$$U_V(Z \leqslant Z^*) = U_R \quad (Z=0) \tag{16}$$

$$P'_V(Z \leqslant Z^*) = P'_R \quad (Z=0) \tag{17}$$

where U_R and P'_R are flow variables at the right end at the initial condition.

To simulate the worst case, the valve at the right end is shut instantaneously at the time the wave reaches this position.

$$U_V(Z > Z^*) = 0 \tag{18}$$

This equation and the compatibility equation along OV are solved to obtain the value of P_V at the right end.

4.2 Left end

At the left end, two distinct time sequences are considered. As long as the pressure is sufficiently greater than the external pressure, the flow will be choked and

$$U_V = -1 \tag{19}$$

Treating the outflow at the broken end when choking occurs as isothermal is a rough approximation. A very high heat transfer rate from the ambient to the gas would be necessary to keep the temperature of the rapidly expanding gas from falling. However, the loss of gas when the outflow is choked is small in comparison with the total amount of gas lost during the three time regimes because of its short duration. Therefore the inaccuracy of this assumption does not affect the computation appreciably.

When the pressure falls to the level of external pressure, the condition used is

$$P'_V = P'_A \tag{20}$$

4.3 Other boundary conditions

Other boundary conditions which may be used with the model are:

(i) prescription of the static pressure as a function of time.

(ii) prescription of the velocity as a function of time. This may be used to simulate valve closure.

The other dependent variable can then be obtained by using the appropriate compatibility equation.

5. Initial conditions

The initial condition is the steady state in the pipeline prior to the initiation of unsteady flow. Neglecting $\ln(P_{IN}/P)^2$ in comparison with $4fx/d$ in long

pipelines (see eq. (6.42) of Ref. [6]), the initial distributions of pressure and velocity in steady isothermal flow are given approximately by

$$P'(X, Z=0)=P'_{IN}\left(1-\frac{4fU_{IN}^2}{D'}X\right)^{1/2} \tag{21}$$

$$U(X, Z=0)=D_{IN}U_{IN}/P'(X, Z=0) \tag{22}$$

6. Stability and accuracy criteria

The time step was chosen in accordance with the Courant–Friedrichs–Lewy stability criterion which requires that

$$\Delta Z \leqslant \frac{\Delta X}{1+|U|} \tag{23}$$

Eighty percent of this maximum allowable time step was used for the computations.

An accuracy criterion based on the law of conservation of mass, defined by Flatt [4] was used in this work. The accuracy criterion is defined as

$$\varepsilon=\frac{(\text{Mass in pipe at time } t)-(\text{Mass in pipe at time } t+\Delta t)}{(\text{Rate of mass outflow at both ends})\Delta t} \tag{24}$$

The ideal value is 1. Hence, the error is

$$e=\varepsilon-1 \tag{25}$$

Flatt [4] introduced a factor K_f by which the friction terms of the compatibility equations are multiplied for the boundary grid point when the flow is sonic. Using the value $K_f=1$ leaves the relations unchanged, whereas $K_f=0$ indicates that the viscous terms are completely omitted.

He found that the singularity at the broken end during critical flow which was discussed in Ryhming's paper [3] caused greater error in the computation when $K_f=1$ than $K_f=0$.

7. Numerical schemes

The equation for the characteristic curves and compatibility relations have been derived following standard procedures. However, the actual numerical implementation of the method of characteristics is not standard. Linear or quadratic interpolation may be used to obtain values of dependent variables at the feet of OV and TV characteristics at the old time level. Also the characteristics may be assumed to be straight or the effect of their curvatures may be considered as suggested by Flatt [7].

Three numerical schemes used in this work are:

(i) linear characteristics and linear interpolation;
(ii) linear characteristics and quadratic interpolation; and
(iii) curved characteristics and quadratic interpolation

A more detailed description of the computation can be found elsewhere [8].

8. Results and discussion

FORTRAN programmes written for the three schemes mentioned above were run on a SWAN AT 286/12 IBM Compatible Personal Computer with a math co-processor using a WATFOR 87 compiler.

The physical case to which the programmes were applied is an underwater pipeline of length 145 km, internal diameter 0.87 m, inlet pressure 133 atm, outlet pressure 55 atm, gas temperature $T_0 = 281$ K, and flow rate about 650 kg/s. The outside pressure $P_0 = 6$ atm (corresponding to 50 m depth). The pipeline is filled with natural gas having a ratio of specific heats $\gamma = 1.3$ and specific gas constant $R = 428.2$ J/kg · K. This was the case considered in references [1], [2] and [4]. The flow in the pipeline is initially steady and isothermal until time $t = 0$ when the pipe is completely broken suddenly at the high pressure end. A constant friction factor $f = 0.0018$ which gives a pressure drop of 78 bars for the steady flow before breakage, was used in the computation of the unsteady flow.

8.1 Comparison of the three schemes

Table 1 shows the errors and computing time for various number of grid points when the unsteady flow process had taken place for 100 seconds. The effect of the magnitude of K_f can be seen. When $K_f = 1$, greater magnitudes of error were obtained and the computation time were higher than when $K_f = 0$ as was observed by Flatt [4]. Therefore the viscous term was omitted in the compatibility equation ($K_f = 0$) for the left boundary grid point when the flow there was critical, in subse quent computations as was suggested by Flatt [4].

TABLE 1

Comparison of error and computation time for the time interval $t = 0$ to $t = 100$ s for the three numerical schemes for various numbers of grid points

Number of grid points	Value of K_f	Error, e at $t = 100$ s			CPU Time (s)		
		LCLI[a]	LCQI[b]	CCQI[c]	LCLI[a]	LCQI[b]	CCQI[c]
201	0	0.357	0.429	0.432	69.92	75.74	83.04
	1	0.967	1.033	0.880	89.42	92.71	119.91
401	0	0.228	0.231	0.233	251.40	280.56	309.73
	1	0.837	0.671	0.669	282.64	310.39	342.52
801	0	0.146	0.124	0.124	966.96	1087.74	1202.59
	1	0.437	0.334	0.330	1148.08	1278.04	1296.90
1601	0	0.088	0.066	0.066	3927.39	4289.46	4745.56
	1	0.231	0.170	0.169	4431.55	4564.58	5223.91

[a] LCLI = Linear Characteristic and Linear Interpolation.
[b] LCQI = Linear Characteristic and Quadratic Interpolation.
[c] CCQI = Curved Characteristic and Quadratic Interpolation.

The higher the number of grid points, the smaller the error for each of the three schemes as expected. At a higher number of grid points the two numerical schemes with quadratic interpolation gave lower errors than the scheme with linear interpolation.

The magnitudes of errors shown in Table 1 may not give a fair assessment of the accuracy of the numerical method employed in this work. A global error criterion (in time) rather than the local error criterion given in eq. (24), may be better. Even the numerical evaluation of eq. (24) is in itself sensitive to numerical accuracy.

Figure 3 shows the comparison of mass flow rate at the broken end predicted with the three numerical schemes using 401 grid points. Since the results predicted with the two schemes using quadratic interpolation agree very closely, it is better to use the linear characteristics with quadratic interpolation scheme because the computer time is lower.

The effect of the curvature of the characteristics is not as important in this work as it was in the work of Flatt [4, 7]. Since the value of the isothermal acoustic velocity (c) remains constant for isothermal flow, the changes in the slopes of the characteristics OV or TV ($u \pm c$) are caused only by changes in

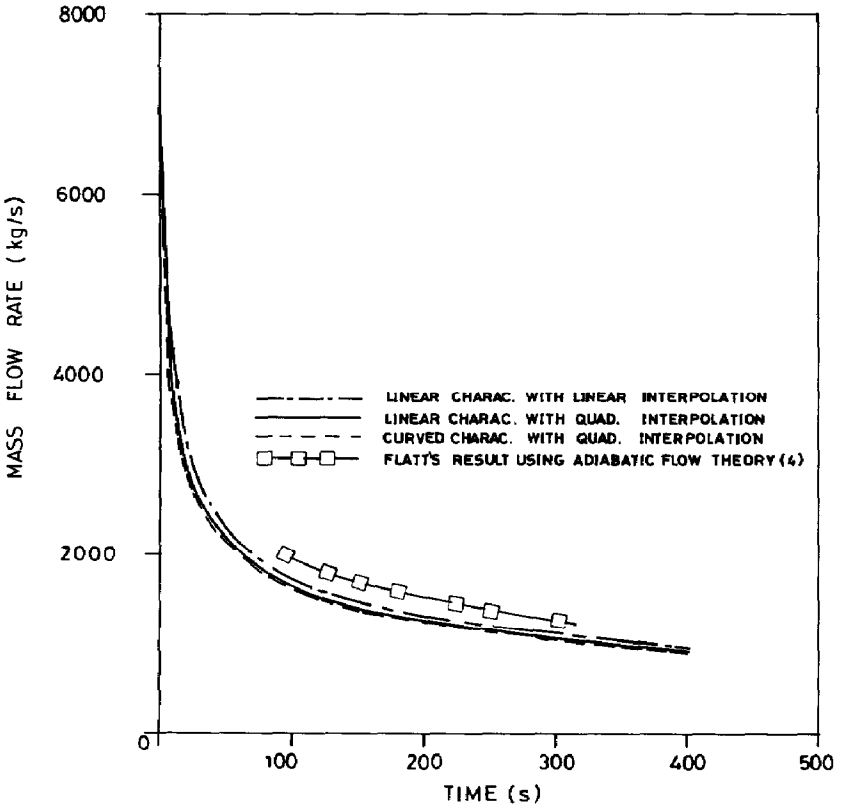

Fig. 3. Comparison of mass flow rate at the ruptured end predicted with the three numerical schemes using 401 grid points. The result obtained by Flatt using adiabatic flow theory is also shown.

magnitude of velocity which are small especially for a fine grid. This is unlike the case of adiabatic flow in which the reciprocal slope of the characteristics are $(u \pm a)$ and both velocity and isentropic acoustic velocity (a) change between T and V and O and V thereby making the slopes vary appreciably.

Secondly an isothermal flow has only two families of characteristics whereas an adiabatic flow has three families of characteristics.

8.2 Test cases

Since a laboratory test of this type of problem cannot be performed in view of the enormous length/diameter ratio, no experimental results are available to test the model. It is necessary to find some other means to assess the model. Ryhming [3] gave the closed form solution of frictionless unsteady isothermal flow obtained during the early time regime when initially there is no flow in the pipe as

$$U=\frac{X}{Z}-1 \tag{26}$$

for the geometry being considered.

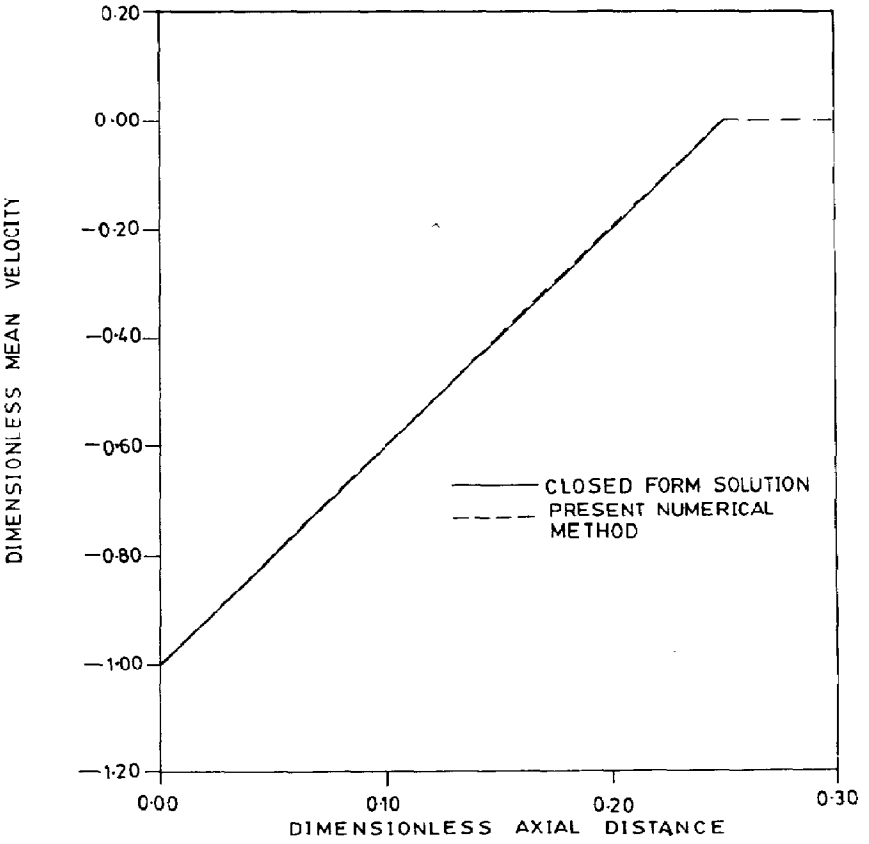

Fig. 4. Comparison of velocity distribution in a pipeline at $Z=0.25$ predicted with the model for unsteady frictionless isothermal flow following sudden break in the pipeline, with result obtained from closed form solution.

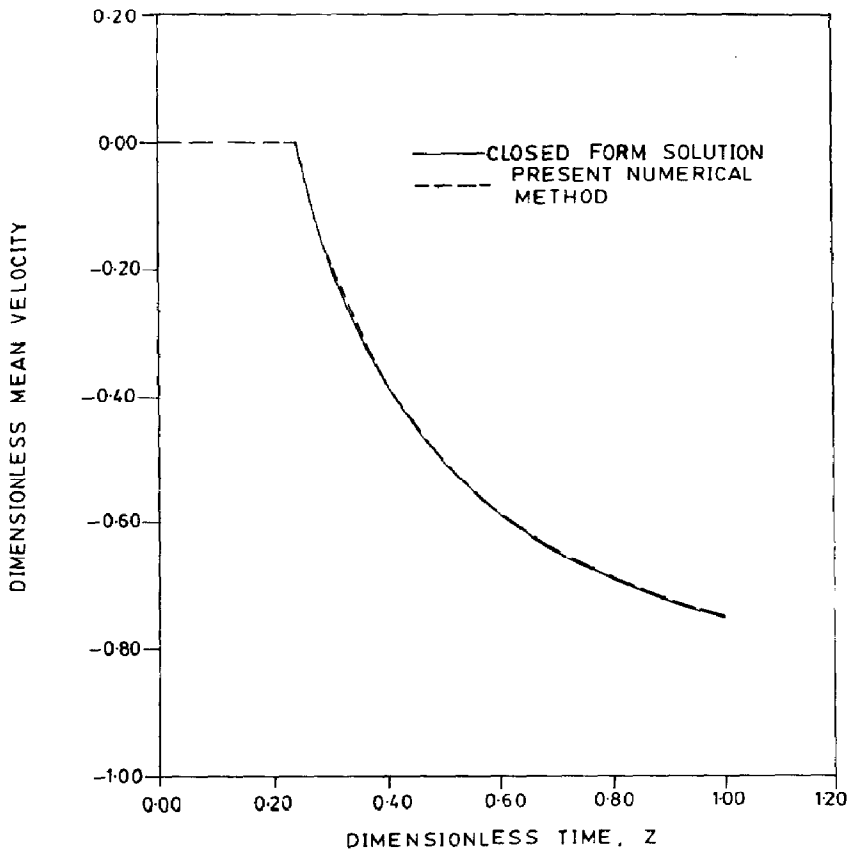

Fig. 5. Comparison of variation of velocity with time at $X=0.25$ predicted with the model for unsteady frictionless isothermal flow following sudden break in a pipeline, with the result obtained from closed form solution.

This solution is applicable for $X \leqslant Z$. For $X > Z$ the velocity $U=0$, since the expansion wave causing leftward flow to the ruptured end has not arrived at that point yet. Figures 4 and 5 show comparisons of results predicted with the model with the closed form solution when the pipe was initially filled with natural gas at dimensionless pressure of 22.17. The agreement of the results predicted with the model with the closed form solution is excellent.

In the second test case, the pipeline was loaded to a dimensionless pressure of 22.17 (with reference to ambient pressure of 6 atm at the pipeline depth) and a diaphragm separates the left end from a lower pressure reservoir of pressure 9.05. The diaphragm at the left boundary is punctured suddenly at time $t=0$. After the transients have died out, the flow obtained should coincide with steady isothermal flow as in eqs. (21) and (22). The pressure and velocity distribution in the pipeline at various times, predicted with the model are shown in Figs. 6 and 7. The pressure and velocity distributions at $t=10{,}000$ s agree quite well with the steady state solutions, considering the fact that coarse grids were used in the computation.

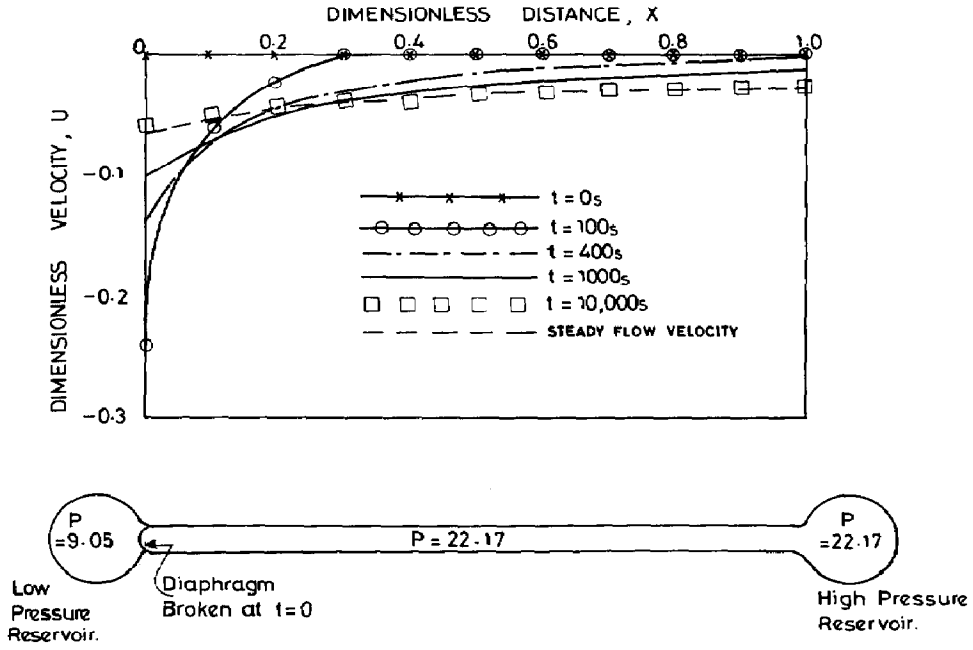

Fig. 6. Velocity distribution at various times for a pipeline linking two reservoirs (101 grid points were used in the computation).

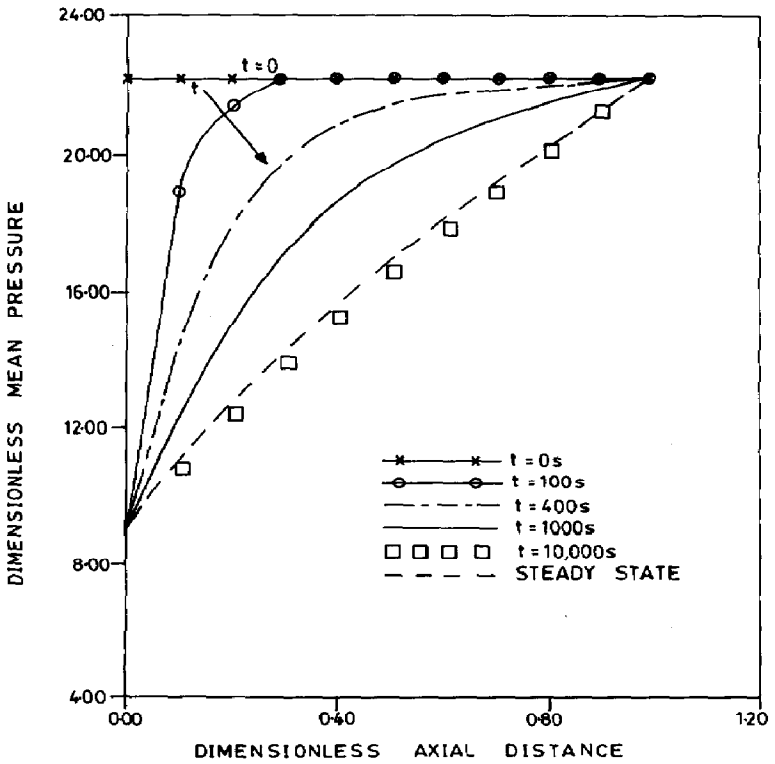

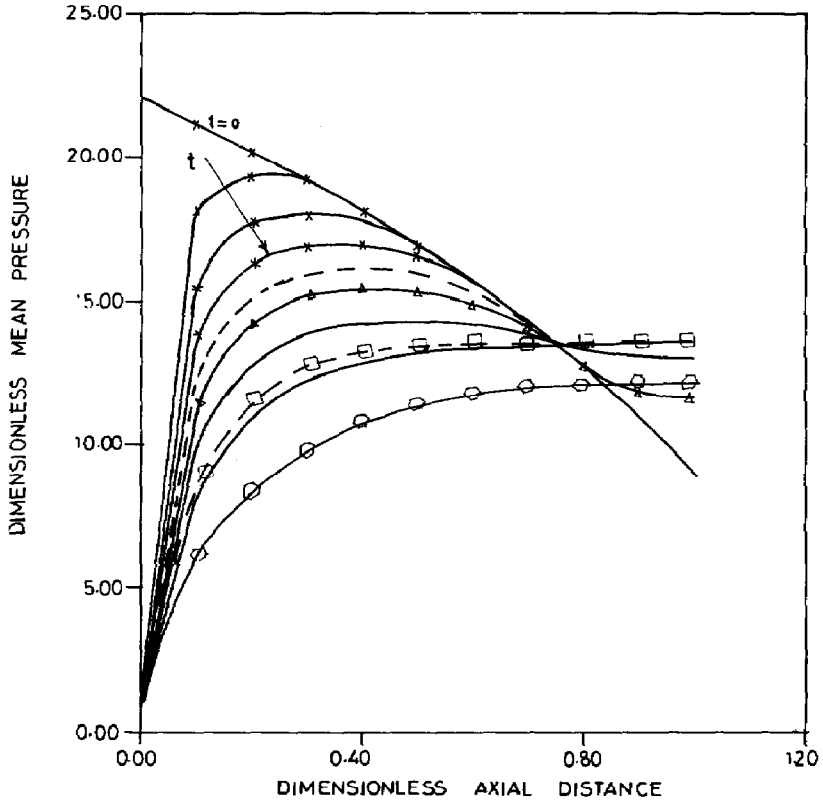

Fig. 8. Pressure distribution in the pipeline after rupture, predicted using 401 grid points, parameter: $t=0$, 100, 200, 300, 400, 500, 700, 900, 1000, 2000 s.

8.3 More results for the North Sea gas pipeline

The pressure distribution in the pipeline at various times after rupture are shown in Fig. 8. It is interesting to see that the pressure does not change at dimensionless distance of 0.75 from the broken end for a very long time (at least 1000 seconds). In Flatt's result, such a point can be seen at a distance of 0.68 from the broken end in his adiabatic flow analysis for the case in which the valve at the low pressure end was closed at $t=0$. If the pressure in the pipeline were monitored at such a point there would be no appreciable change in the indicated pressure for a very long time, even after the expansion wave initiated at the rupture has reached that point.

The variation of pressure at the left and right ends with time are shown in Figs. 9 and 10. The pressure starts to rise at the right end as soon as the expansion wave gets there and the valve is shut and peaks at a valve of about 13.7 before it begins to fall.

Shown in Fig. 3 is the mass flow rate out of the broken end between $t=100$ s and $t=300$ s obtained by Flatt [4] using unsteady adiabatic flow theory. The

Fig. 7. Pressure distribution at various times for a pipeline linking two reservoirs (101 grid points were used in the computation).

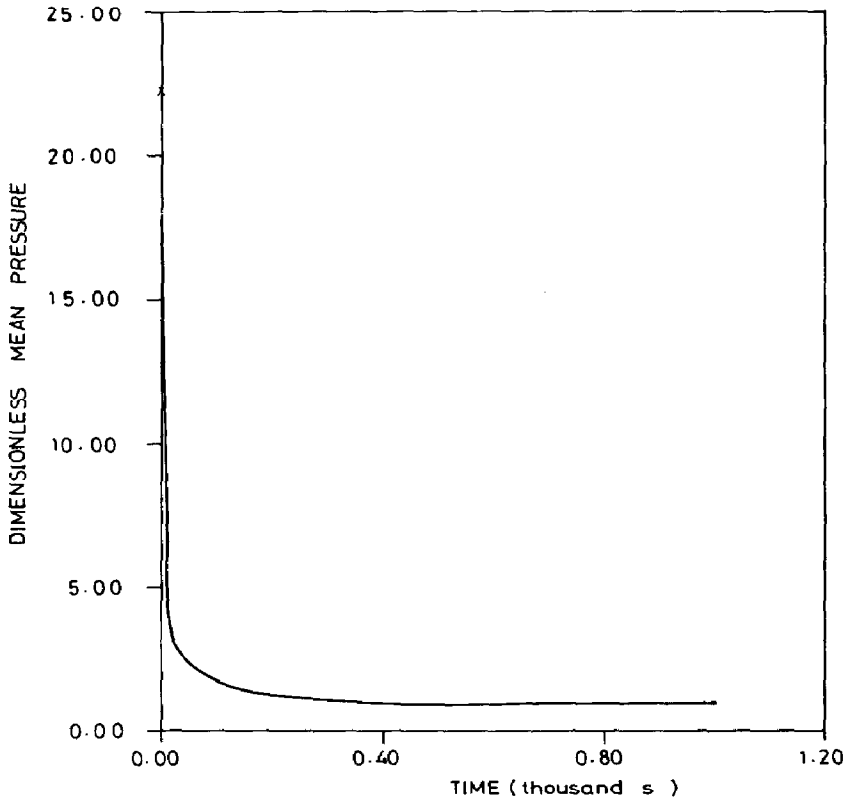

Fig. 9. Predicted pressure variation with time at the break point.

results obtained in this present work using isothermal flow theory are lower than Flatt results by about 18%. This is partly due to the fact that the isentropic sonic velocity is higher than isothermal sonic velocity.

Figure 11 shows the dimensionless mass flow rate predicted using different number of grid points. It took 7 h, 57 min and 17 s to compute the flow for a real-flow time of 2,000 s using 401 grid points. Using 201 and 101 grid points it took 5 h, 54 min and 3 h, 45 min and 61 s to compute the flow for real-flow times of 7,000 and 20,000 seconds, respectively. These results agree quite well with that obtained by Lang and Fanneløp [2] using spectral collocation method with Legendre polynomials, as can be seen in Fig. 11.

From Fig. 3, the mass flow rate out of the broken end was initially 7,550 kg/s. By 100 s the mass flow had reduced to 1630 kg/s. After 5 h and 30 min the mass flow rate was less than 15 kg/s, as can be seen in Fig. 11.

9. Conclusions

A mathematical model based on unsteady isothermal flow theory and solved by the method of characteristics has been presented. The model predicts results consistent with the predictions of other workers.

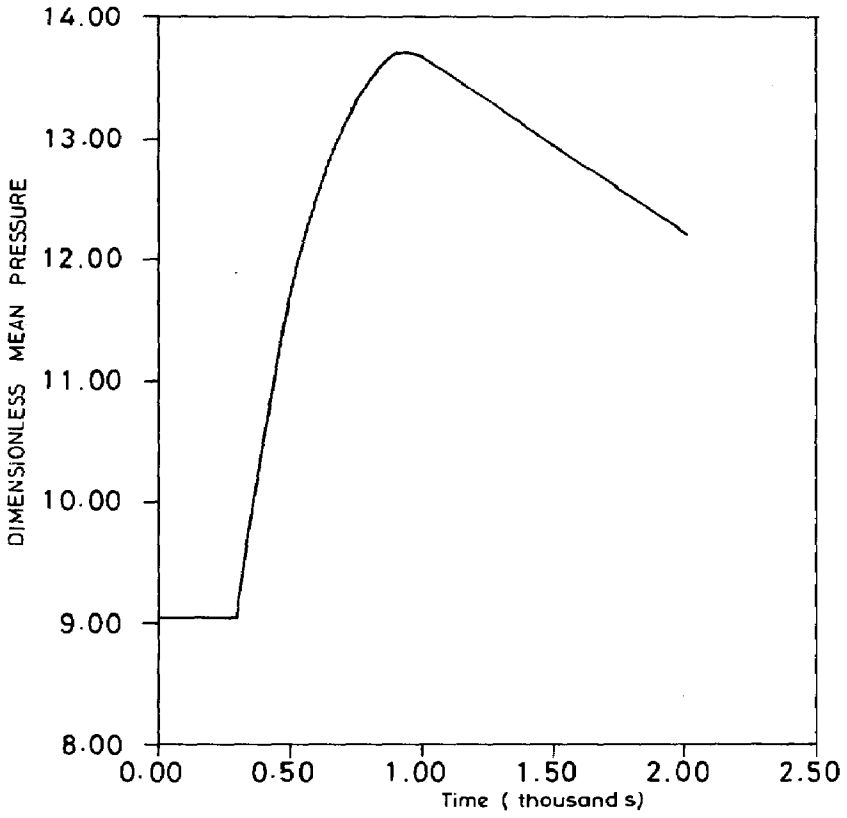

Fig. 10. Predicted pressure at the right hand end of the pipe segment.

Flow rate predicted at the broken end of the pipe is lower than that of adiabatic flow theory by about 18% but it agrees quite well with that of Lang and Fanneløp obtained using a method of weighted residuals to solve unsteady isothermal flow equations.

At a dimensionless distance of 0.75 from the broken end of the pipeline segment, the pressure does not change for a very long time.

The curvature of the characteristics is not as pronounced in isothermal flow as it is in adiabatic flow. Therefore it is not necessary to include the effect of the curvature of the characteristics in the computation of unsteady isothermal flows.

This model is useful in analysing other unsteady flows associated with pipeline operations, such as controlled venting to the atmosphere prior to shutdown or repair, and sudden changes in pressure at either end of the pipeline. The waves generated in these operations cannot be as strong as the waves associated with pipeline rupture. Hence the model can handle such situations easily. All that is necessary is to use appropriate boundary conditions.

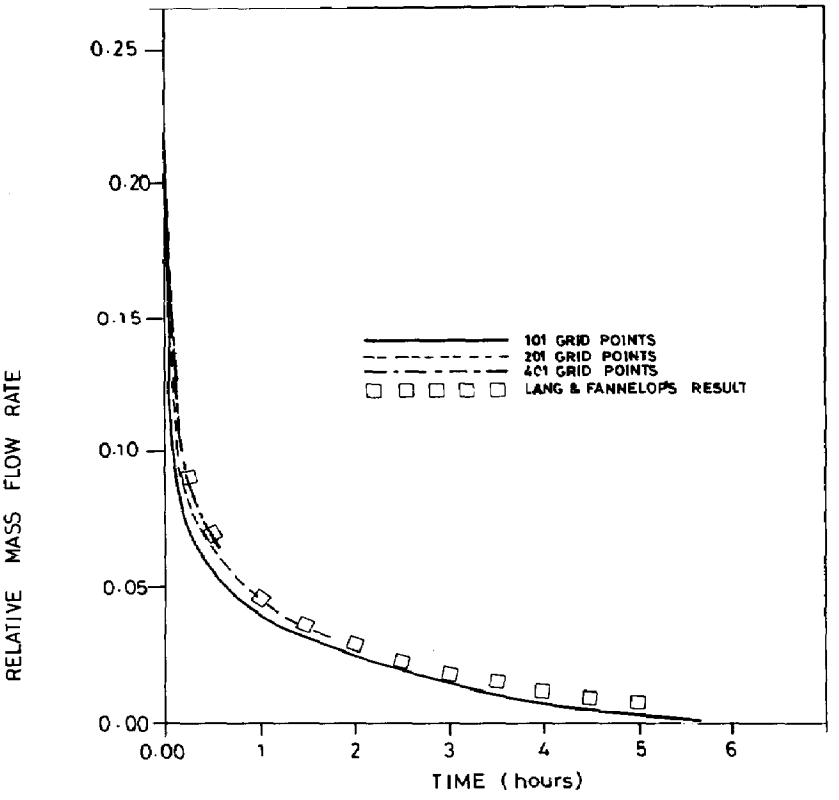

Fig. 11. Relative flow rate ($\dot{m}$ (0, t)/$\dot{m}$ (0, $t=0$)) at the break as a function of time.

Acknowledgements

The provision of computing facilities for this project by the University of Ilorin Computer Centre at first and later by the Faculty of Engineering is gratefully acknowledged. The principal author is grateful for the award of Senate Research Grant No. 8:15:303 at the University of Ilorin while this project was carried out.

Notation

Where applicable non-dimensional forms are given.

Roman

c		Isothermal speed of sound
		Reference velocity
d	$D'=d/l_0$	Pipe diameter
e		Error

f		Friction factor
F	$F'=Fl_0/c^2$	Friction force per unit mass
I, M, N, V		Grid points
l_0		Pipe length. Reference length
O, T		Feet of characteristics
P	$P'=P/P_0$	Mean pressure at a pipe cross-section
P_0		Ambient pressure. Reference pressure.
R		Specific gas constant
t	$Z=tc/l_0$	Time
T_0		Ambient temperature. Reference temperature
u	$U=u/c$	Velocity
x	$X=x/l_0$	Axial distance
Z^*		Non-dimensional time taken for wave to travel from the left end to the right end

Greek

Δt	ΔZ	Time step size
Δx	ΔX	Spatial grid size
ε		Accuracy criterion
ρ	$D=\rho/\rho_0$	Density
ρ_0		Density of gas at the reference pressure and temperature

Subscripts

IN	Initial conditions at left end of pipeline
O	Foot of characteristic OV
OV	Along characteristic OV
R	Dependent variables at right end
T	Foot of characteristic TV
TV	Along characteristic TV
V	Grid point V

Superscripts

	Normalized with respect to appropriate reference value

Operators

D/DZ	Substantial derivative
$\delta_+/\delta Z$	Differentiation following characteristic having reciprocal slope $(U+1)$
$\delta_-/\delta Z$	Differentiation following characteristic having reciprocal slope $(U-1)$

References

1 T.K. Fanneløp and I.L. Ryhming, Massive release of gas from long pipelines, J. Energy, 6 (1982) 132–140.

2 E. Lang and T.K. Fanneløp, Efficient computation of the pipeline break problem. 3rd Symp. on Fuid-Transients in Fluid Structure Interaction. FED, Vol. 56, ASME Winter Annual Meeting, Boston, MA, 1987.
3 I.L. Ryhming, On the expansion wave problem in a long pipe with wall friction, J. Appl. Math. Phys. (ZAMP), 38 (1987) 378–390.
4 R. Flatt, Unsteady compressible flow in long pipelines following a rupture, Int. J. Num. Methods Fluids, 6 (1986) 83–100.
5 J.A. Olorunmaiye and J.A.C. Kentfield, Numerical simulation of valveless pulsed combustors, Acta Astronautica, 19 (1989) 669–679.
6 A.H. Shapiro, The Dynamics and Thermodynamics of Compressible Fluid Flow, Vol. I, Wiley, New York, 1953.
7 R. Flatt, A singly-interactive second-order method of characteristics for unsteady compressible one-dimensional flows, Commun. Appl. Num. Methods, 1 (1985) 269–274.
8 N.E. Imide, Computation of Unsteady Isothermal Flow in Long Natural Gas Pipelines. M. Eng. Thesis, University of Ilorin, Ilorin, Nigeria, Sept. 1991.